Biochimica et Biophysica Acta 1818 (2012) 2529–2535

Contents lists available at SciVerse ScienceDirect

Biochimica et Biophysica Acta

journal homepage: www.elsevier.com/locate/bbamem

Ion solvation and structural stability in a sodium channel investigated by molecular dynamics calculations

Hu Qiu, Rong Shen, Wanlin Guo *

State Key Laboratory of Mechanics and Control of Mechanical Structures, the Key Laboratory for Intelligent Nano Materials and Devices of MoE, Institute of Nano Science, Nanjing University of Aeronautics and Astronautics, Nanjing 210016, China

ARTICLE INFO

Article history:
Received 18 November 2011
Received in revised form 23 May 2012
Accepted 4 June 2012
Available online 12 June 2012

Keywords:
Sodium channels
Molecular dynamics
Structural stability
Ion hydration

ABSTRACT

The stability and ion binding properties of the homo-tetrameric pore domain of a prokaryotic, voltage-gated sodium channel are studied by extensive all-atom molecular dynamics simulations, with the channel protein being embedded in a fully hydrated lipid bilayer. It is found that Na^+ ion presents in a mostly hydrated state inside the wide pore of the selectivity filter of the sodium channel, in sharp contrast to the nearly fully dehydrated state for K^+ ions in potassium channels. Our results also indicate that Na^+ ions make contact with only one or two out of the four polypeptide chains forming the selectivity filter, and surprisingly, the selectivity filter exhibits robust stability for various initial ion configurations even in the absence of ions. These findings are quite different from those in potassium channels. Furthermore, an electric field above 0.5 V/nm is suggested to be able to induce Na^+ permeation through the selectivity filter.

1. Introduction

Selective ion conduction via ion channels across cell membrane plays an essential role in neural signal transduction. The pioneering electrophysiological studies by Hille [1–6] and Armstrong [2,7–9] have explored the permeability and selectivity of the eukaryotic channels that are Na^+-, K^+- or Na^+/K^+-selective since the early 1970s, with the aid of patch-clamp techniques. They suggested that these ion channels consist of a long narrow pore, and thirty years later, this idea was confirmed by the first crystal structure of the bacterial KcsA K^+ channel [10,11]. Since then, a variety of K^+-selective channels have also been reported, such as the bacterial MthK [12] and KvAP [13] channels, as well as the eukaryotic Kv1.2 channel [14]. In K^+ channels, the selectivity filters share a highly conserved sequence of TVGYG and form a one-dimensional ion conduction pathway. From the extracellular to the intracellular side of the selectivity filter, four explicit K^+ ion binding sites (numbered S1 to S4) are formed by two layers of oxygen atoms provided by the backbone carbonyl groups of the TVGY sequence and by the side chains of the Thr residues. K^+ ion in the selectivity filter presents in a dehydrated form and water oxygen atoms originally within its coordination shell are replaced by the eight protein oxygen atoms surrounding each site. Ions can instantaneously occupy the S1 and S3 sites or the S2 and S4 sites in the selectivity filter, with the rest of the sites being occupied by waters [15]. Molecular dynamics (MD) simulations show that K^+ conduction across the selectivity filter takes place by a concerted motion via the alternation of these two configurations [16]. In addition to the K^+-selective channel, the crystal structures of another type of ion channels from *Bacillus cereus* called NaK that can conduct both Na^+ and K^+ ions were also reported [17,18]. Based on these atomic structures, numerous computational studies were carried out to study the conduction, selectivity, and gating of the K^+ and NaK channels [15,16,19–30].

For the selective conduction of sodium across membranes, the main mediators are voltage-gated sodium channels. Recently, a number of prokaryotic sodium channels have been identified, providing opportunities for structural and functional characterization of sodium channels. The first identified and most well-characterized prokaryotic sodium channels are NaChBac from *Bacillus halodurans* [31], which share a high degree of sequence identity (22 to 69%) with sodium channels from other bacterial homologues [32]. The possibility to express functional NaChBac in both mammalian cells and in bacterial cultures has attracted a number of studies to characterize its conduction [31], gating [33,34] and selectivity [35]. However, the detailed structure–function relationship of sodium channels is yet to be understood due to the lack of high resolution crystal structure. It is the finding of the crystal structure of a NaChBac homologue, NavAb from *Arcobacter butzleri*, that provides for the first time the possibility to study the function of a Na^+-selective channel at the atomic scale [36]. Unlike the K^+ channel, the selectivity filter of NavAb channel has a conserved sequence of $_{175}$TLESW$_{179}$ and forms a much wider channel pore than the K^+ channels, implying that Na^+ ions inside the selectivity filter should have more waters of hydration than K^+ in K^+ channels. The larger channel pore also implies that ions inside the filter may not take a single-file configuration and ion permeation through the NavAb channel may not occur in a strictly concerted manner as the K^+ channel does. Shortly before the submission of this manuscript, a molecular dynamics study

* Corresponding author. Tel.: +86 25 84891896; fax: +86 25 84895827.
E-mail address: wlguo@nuaa.edu.cn (W. Guo).

0005-2736/$ – see front matter © 2012 Elsevier B.V. All rights reserved.
doi:10.1016/j.bbamem.2012.06.003

by Carnevale et al. confirmed that about four waters were found to hydrate each Na^+ ion inside the NavAb selectivity filter and ion conduction did not adopt a single-file manner [37]. Furthermore, only three potential ion binding sites are detected along the ion permeation pathway of the NavAb selectivity filter.

In this study, we carried out systematic molecular dynamics simulations based on the recently reported crystal structure of the NavAb channel. The simulation results show that the channel protein can be stable for simulations with all ion configurations we studied within 10 ns MD simulations and water molecules can diffuse freely across the selectivity filter between the cavity and extracellular solution. Large motions are found for Na^+ ions inside the selectivity filter, suggesting that ions cannot bind to the channel protein as stably as in the K^+ channels. Our results further show that the coordination numbers of Na^+ ions at $Site_{HFS}$ and $Site_{IN}$ are nearly identical (~5.5), while the hydration numbers of Na^+ ions at $Site_{HFS}$ (~2.5) and $Site_{IN}$ (~5.5) deviate from each other significantly. This fact indicates that about three protein oxygen atoms participate in coordinating the ion at $Site_{HFS}$, provided by the side chains of the residue Glu177, while only one protein oxygen atom is found to occasionally bind with the ion at $Site_{IN}$. Furthermore, under an electric field exceeding 0.5 V/nm, the conduction of Na^+ through the NavAb channel takes place in our simulations.

2. Methods

The NavAb tetramer was prepared using VMD [38] based on the recently published structure from the protein data bank (PDB code: 3RVY) [36]. The voltage-sensing domain (residue ID 1–113) of the NavAb channel was removed for the computational efficiency and to ensure a tight contact between the protein and the lipid bilayer. Default ionization states were used for all amino acids. The protein was then embedded in a palmitoyl-oleoylphosphatidylcholine (POPC) bilayer and solvated by adding water molecules on both sides of the membranes (Fig. 1). Na^+ and Cl^- ions were added to the solution to obtain an electro-neutral system with an ion concentration of 0.1 M. The finial system contains totally 45,561 atoms, including the NavAb structure containing 7132 atoms, 119 POPC lipid molecules, 7491 water molecules and 9 Na^+ ions and one Cl^- ion. About fifty water molecules were originally located in the cavity of the NavAb channel to stabilize the protein during the initial period of MD simulations. The membrane normal was oriented along the *z* axis, with the center of mass of the C_α atoms of the selectivity filter residues being set as the zero point.

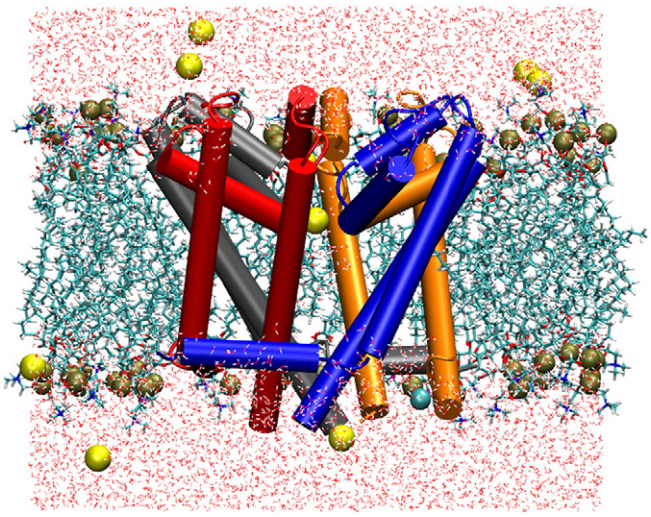

Fig. 1. The simulation system. Four monomers of NavAb (blue, red, black and orange) are shown in cartoon representation and were embedded in a POPC lipid bilayer (cyan sticks) surrounded by water (red dots). Some of the lipid molecules are not shown for clarity. Na^+ (yellow), Cl^- (cyan), and phosphorus atoms (brown) are shown in vdW spheres, respectively.

All MD simulations were performed by the program NAMD2 [39] using the CHARMM27 force field [40] for the protein and lipids, and the TIP3P model [41] for water. L-J parameters for ions were chosen in accord with Roux and Berneche [42]. Periodic boundary conditions were applied in all directions. The long-range electrostatic interactions were calculated with the particle mesh Ewald (PME) method [43]. Langevin dynamics and the Nose–Hoover Langevin piston method were chosen to maintain the temperature at 310 K and the pressure at 1 atm [44] respectively. In our simulations, a time step of 1 fs was used and data were recorded every 1 ps. Beginning with 1000 steps energy minimization, the system was simulated for 200 ps, with all protein atoms being fixed to remove the gap between the protein and lipids. Then all the ion configurations listed in Table 1 were constructed. After that, gradually decreasing harmonic restraints were applied to the protein atoms. Finally, the whole system was simulated for 10 ns with no restraints. Pore radius profiles were calculated with the code HOLE [45].

The starting structure for transport simulations of Na^+ ion across the channel pore was taken from the equilibrated configuration from Sim4, in which only one Na^+ at $Site_{IN}$ occupies the pore. The ion conduction process was induced by applying various levels of constant force to each ion inside the ion conducting pore in the upward direction, simulating the driving by transmembrane potential. The field (force) was applied to the ions only to avoid the protein distortion by the large electric field. A number of previous MD studies have used electric field or force to induce ion conduction in K^+ [46–48] and NaK [29,30] channels and generated reasonable results. The C_α atoms of Gly129 residues, far from the selectivity filter, were restrained with a harmonic spring of 2 kcal/mol/Å^2 to avoid the drift of the protein. During these simulations, the Langevin dynamics used for maintaining a constant temperature and pressure was applied only to the lipid membrane, to prevent the presence of an extra, artificial friction force introduced by the Langevin dynamics affecting the transport property of the conducted ion [49].

The one-dimensional potential of mean force (1D PMF) for Na^+ ion conduction across the selectivity filter was calculated using umbrella sampling [50], with the starting configuration also extracted from the equilibrated configuration of Sim4. The width of each umbrella window was 0.5 Å. A biasing potential of 20 kcal/mol/Å^2 was applied on the z coordinate of the Na^+ ion in each window. In order to obtain the 1D PMF, we first placed a single ion inside the selectivity filter and then carefully monitored the channel occupancy during the umbrella sampling. If other ions entered the selectivity filter, the MD trajectory will not be used and the simulation was carried out again until a trajectory with only one ion inside the selectivity filter during the whole simulation was obtained. All simulations were conducted for 1 ns, with the last 900 ps for data analysis. Umbrella histograms were then unbiased and combined using the weighted histogram analysis method (WHAM) to obtain the 1D PMF profile [51].

3. Results and discussion

3.1. Structure and pore profile of the selectivity filter

Similar to the K^+ and NaK channels, the NavAb channel protein is also tetrameric and has a central conduction pore formed together by the four monomers, which consists of an outer vestibule, a selectivity filter, a central cavity and an activation gate [36]. However, the architecture of ion binding sites in the selectivity filter of the NavAb channel is different from those of the K^+ and NaK channels, in which the binding sites are formed mostly by the backbone carbonyl groups of the selectivity filter residues pointing directly into the channel pores. For the

Table 1
Summary of simulations.

ID	Initial configuration				Stable configuration				Backbone RMSD for protein (Å)	RMSD for filter (Å)
	$Site_{HFS}$	$Site_{CEN}$	$Site_{IN}$	Cavity	$Site_{HFS}$	$Site_{CEN}$	$Site_{IN}$	Cavity		
Sim1									1.33 ± 0.09	0.59 ± 0.04
Sim2	Na						Na		1.39 ± 0.08	0.66 ± 0.07
Sim3		Na					Na		1.34 ± 0.12	0.56 ± 0.05
Sim4			Na				Na		1.45 ± 0.12	0.56 ± 0.04
Sim5				Na				Na	1.44 ± 0.13	0.63 ± 0.07
Sim6	Na		Na		Na		Na		1.68 ± 0.15	0.87 ± 0.22
Sim7[a]	Na		Na	Na	Na		Na		1.59 ± 0.09	1.06 ± 0.08

Sites occupied by Na^+ ions are indicated by "Na".
RMSDs (mean ± s.d.) for backbone atoms of the protein and all non-hydrogen atoms of the selectivity filter from the crystal structure were averaged over the final 8 ns of each MD simulation.
[a] In this simulation, Na^+ ion initially at $Site_{HFS}$ soon escapes to the solution, and meanwhile, the two remaining Na^+ ions at $Site_{IN}$ and Cavity move upward to bind at the $Site_{HFS}$ and $Site_{IN}$, respectively.

NavAb channel, three potential ion binding sites were detected: $Site_{HFS}$ formed by the side chains of Glu177, $Site_{CEN}$ formed by the carbonyl groups of Leu176, and $Site_{IN}$ formed by the carbonyl groups of Thr175 (Fig. 2A). At $Site_{HFS}$, the backbone carbonyl groups point outward the pore lumen, while the side chains of Glu177 point inward to the conducting pore to bind with adjacent ions. At $Site_{CEN}$, the backbone carbonyl groups of Leu176 are also not exposed to the pore apparently, suggesting that Na^+ may not bind at this site stably. However, at $Site_{IN}$, the residue Thr175 orients its backbone carbonyl group toward the pore lumen to coordinate ions.

It has been suggested that the channel pore of the NavAb channel is significantly wider and shorter than the KcsA K^+ channel [36]. This fact implies that ions within the NavAb channel should be highly hydrated, while in the K^+ channels, ions pass through the selectivity filters in nearly fully dehydrated states. The narrowest part of the NavAb selectivity filter is formed by the side chains of Glu177 residues at $Site_{HFS}$ (Fig. 2). Apart from this region, the wider pore allows the hydrated Na^+ ion to diffuse freely within the selectivity filter and exchange between the selectivity filter and the cavity. In addition, the wider and shorter nature of the selectivity filter implies that it may be difficult to unravel the mechanism of the NavAb channel selectivity. Fig. 2B shows the averaged pore radius profiles from three MD simulations with different initial configurations: no ions (dashed line), one ion at $Site_{IN}$ (dotted line) and two ions at $Site_{HFS}$ and $Site_{IN}$ (dashed dotted line). In general, the selectivity filter pore shrinks in most regions during our MD simulations compared to the one from NavAb crystal structure, especially at $Site_{CEN}$. The results also show that the pore radius profile for the simulation without ions is nearly identical to the one with one ion inside the selectivity filter, implying the low flexibility of the channel protein, which will be further discussed below. In addition, comparing to the simulations with less ions (zero or one), we found that the pore size around $Site_{HFS}$ in the simulation with two ions is significantly smaller. This constriction should be attributed to the attraction of the Na^+ ion at this site with the side chain of the negatively charged residue, Glu177.

3.2. Stability of the protein and the selectivity filter

Table 1 lists the simulations conducted in this work with different initial configurations of the ions in the channel pore. At first glance, it is surprising to find that the selectivity filter is quite stable for all ion configurations we investigated during 10 ns MD simulations, even in the absence of ions inside the channel pore (Sim1). When only one Na^+ ion is positioned in the selectivity filter (Sim2–Sim4), the ion will rapidly move to the $Site_{IN}$ and stay at this site. If this ion is placed in the cavity initially, it can diffuse freely inside the cavity, and, it does not move to the selectivity filter within our 10 ns simulations (Sim5). In Sim6, two Na^+ ions can stay at $Site_{HFS}$ and $Site_{IN}$ during the whole 10 ns simulation. When three Na^+ ions are placed at $Site_{HFS}$, $Site_{IN}$ and Cavity, receptively (Sim7), the uppermost Na^+ ion initially at $Site_{HFS}$ soon escapes to the bulk solution, and meanwhile, the lower two ions come to occupy $Site_{HFS}$, $Site_{IN}$. The ion configuration inside the pore is then identical to that of Sim6. The robust stability of NavAb is in sharp contrast to the situations for the K^+ [20,52,53] and NaK [29,30] channels, in which the selectivity filters can only be stable for certain ion arrangements and the absence of ions will destabilize the structure of the selectivity filter.

Table 1 also gives the average root mean square deviations (RMSDs) of the backbone atoms of the NavAb protein and all the non-hydrogen atoms of the selectivity filter during MD simulations. In general, for all simulations, the backbone RMSDs are less than 1.7 Å, and the RMSDs for the selectivity filters are lower than the backbone RMSDs for the whole protein. Furthermore, the RMSDs for 10 ns simulations without ions (Sim1) or with only one ion (Sim2–Sim5) occupying the pore are found to be a little lower than those for the case of two (Sim6) or three (Sim7) ions in the pore. In detail,

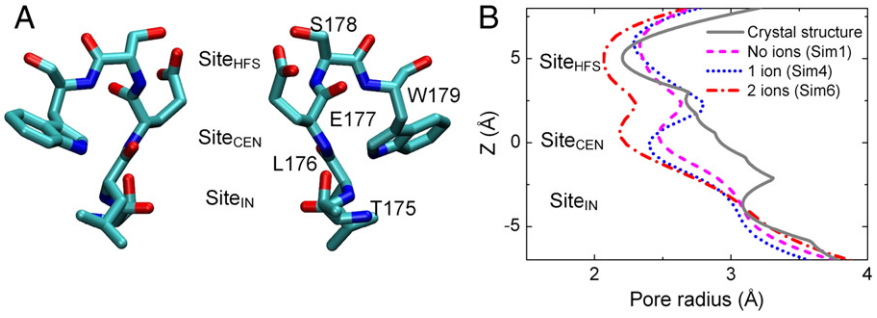

Fig. 2. Pore profile of the selectivity filter of the NavAb channel. (A) The selectivity filter of NavAb. (B) Comparison of pore radius profiles from NavAb crystal structure and from MD simulations. The dashed line, dotted line, and dash dotted line show the average radius of selectivity filter pore of the NavAb channel during the last 6 ns of Sim1 (no ions), Sim4 (one ion at $Site_{HFS}$) and Sim6 (two ions at $Site_{HFS}$ and $Site_{IN}$), respectively. The extracellular side is on the top and the intracellular side is at the bottom.

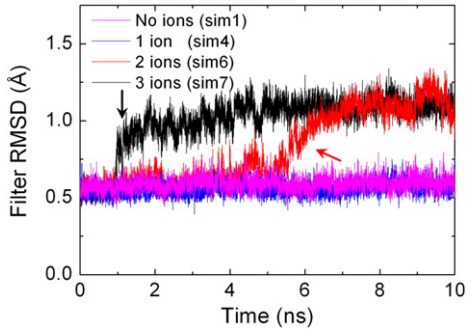

Fig. 3. Drift of the selectivity filter structure from the initial model. The RMSD of all non-hydrogen atoms of the selectivity filter from its starting structure is shown as a function of simulation time for four typical initial ion configurations: no ions (Sim1), one ion at $Site_{IN}$ (Sim4), two ions at $Site_{HFS}$ and $Site_{IN}$ (Sim6), and three ions at $Site_{HFS}$, $Site_{IN}$ and Cavity (Sim7).

Fig. 3 shows the RMSDs for all non-hydrogen atoms of the selectivity filters as a function of simulation time in four typical simulations with the number of ions inside the channel pores ranging from 0 to 3. In general, the low RMSD values (<1.25 Å) indicate that the structure of selectivity filter is stable during 10 ns MD simulations, regardless of the initial ion configurations. It is also found that in the presence of a single ion or no ions, the selectivity filter RMSD fluctuates slightly with an average of ~0.6 Å in the 10 ns MD simulation (Fig. 3, blue and magenta lines). This phenomenon is also observed during the first 5.5 and 1.0 ns for the simulations with two and three ions inside the channel pore, respectively (Fig. 3, red and black lines). However, at about 5.5 ns and 1.0 ns (red and black arrows), the filter RMSDs are increased to ~1.0 Å. Although this jump is not significant and accessible in thermal bath at room temperature, it does to some extent reflect the structural distortion of the selectivity filter. We carefully examined the MD trajectories and found that the larger RMSD is caused mainly by the deflection of the side chains of Glu177 residues when binding with the Na^+ at $Site_{HFS}$. Nevertheless, it should be noted that the demonstrated robust stability of NavAb is obtained based on a low resolution (~2.7 Å) crystal structure and using 10 ns MD simulations. To validate the protein stability in longer simulations, we further conducted a 50 ns MD simulation that was restarted from Sim7 and found that the structure of NavAb selectivity filter is quite stable during the entire simulation (see Fig. S1 in supplementary data). We would expect that further studies with even longer simulations on a higher resolution structure could address this issue more clearly.

To further understand the fluctuations of the channel, we calculated the RMS fluctuations for each residue of the NavAb selectivity filter in Sim6. Considering the asymmetric nature of Na^+ binding, we explicitly define the quadratic fluctuation to be the sum of two terms [54]: (1) the standard mean square atomic fluctuations averaged over the four monomers, $\langle \Delta \mathbf{r}_i^2 \rangle_{\text{fluct}} = \frac{1}{4}\sum_{m=1}^{4}\left(\langle \mathbf{r}_{i,m}^2\rangle - \langle \mathbf{r}_{i,m}\rangle^2\right)$; (2) the mean square deviation of the monomers away from the tetrameric symmetry, $\langle \Delta r_i^2 \rangle_{\text{sys}} = \left(\frac{1}{4}\sum_{m=1}^{4}\langle \mathbf{S}_m \mathbf{r}_{i,m}\rangle^2\right) - \left(\frac{1}{4}\sum_{m=1}^{4}\langle \mathbf{S}_m \mathbf{r}_{i,m}\rangle\right)^2$, where $\mathbf{S}_m$ is a matrix operator that is applied to the monomer A, B, C and D to rotate their positions around the pore axis with 0°, 90°, 180° and 270°, respectively, to obtain the symmetrized average position $\langle \mathbf{S}_m \mathbf{r}_{i,m}\rangle$. For comparison, we divided the MD trajectory of Sim6 into two periods, with the "jump" at the RMSD profile being the demarcation (see Fig. 3, red line): 0–5.5 ns, and 5.5–10 ns. The results are shown in Table 2. In general, it is found that the standard RMS fluctuations for each residue, RMS_{fluct}, are all in the range of 1.00 to 1.50 Å, and that the RMS_{fluct} are nearly identical for these two periods, confirming the robust stability of the structure of the selectivity filter. Furthermore, the residue with

Table 2
RMS fluctuations of the non-hydrogen atoms of the selectivity filter residue calculated from Sim6.

Residue number	0–5.5 ns		5.5–10 ns	
	RMS_{fluct} (Å)	RMS_{sym} (Å)	RMS_{fluct} (Å)	RMS_{sym} (Å)
T175	1.00	0.15	1.07	0.22
L176	1.03	0.04	0.93	0.18
E177	1.25	0.08	1.14	0.32
S178	1.00	0.04	1.00	0.07
W179	1.40	0.09	1.46	0.15

RMS_{flut} and RMS_{sym} represent the standard root mean square fluctuation and root mean square deviation of the monomers away from the tetramer symmetry, respectively. The MD trajectory was divided into two periods for this calculation: 0–5.5 ns and 5.5–10 ns.

the largest RMS_{fluct} was found to be Trp179, which points outward the pore lumen and does not participate in ion binding (see Fig. 2A). This is presumably due to the large fluctuation of the large side chain of this residue that consists of two fused aromatic rings. For the RMS term that reflects the fluctuation of tetrameric symmetry, RMS_{sym}, we found that the value for the first period (0–5.5 ns) is significantly lower than that for the second period (5.5–10 ns), especially for the Glu177, which increases from 0.08 Å to 0.32 Å. Examination of the MD trajectory suggests that the side chains of Glu177 from four monomers are not symmetrical during the second period (5.5–10 ns), due to the binding of Na^+ ions to Glu177 from only one or two monomers (see Fig. 5C). The influence of this binding pattern on the coordination state of Na^+ ion will be addressed detailedly in the following section.

3.3. Solvation and ion binding state for Na^+ ions inside the selectivity filter

Two relatively stable ion binding sites $Site_{HFS}$ and $Site_{IN}$ have been identified in the above discussion and in a recent work [37]. The coordination and hydration states for ions inside the selectivity filter were suggested to be crucial for the selectivity of ion channels [26,27,55]. To study detailedly the coordination states for Na^+ ions at these two binding sites, we calculated the ion-oxygen radial distribution functions (RDFs) for Na^+ ions with respect to total ligands, water oxygen, and protein oxygen, respectively (Fig. 4A and B). The region between the first maximum and minimum in RDF profiles indicates the first coordination shell of ion. In general, the total RDF profiles for ions at $Site_{HFS}$ (Fig. 4A, black line) and $Site_{IN}$ (Fig. 4B, black line) are nearly identical, but the types of oxygen in the first coordination shell deviates significantly from each other. For Na^+ ion at $Site_{HFS}$, some oxygen atoms from the side chains of Glu177 were found to fall within its first coordination shell, leading to an apparent peak in the RDF profile for protein oxygen (Fig. 4A, red line). In contrast, few protein oxygen atoms can be found within the first coordination shell of Na^+ ion at $Site_{IN}$ (Fig. 4B, red line) and the RDF for water oxygen (Fig. 4B, blue line) is almost identical to the total RDF profile (Fig. 4B, black line), suggesting that Na^+ at this site should present in a more highly hydrated state.

The coordination number and hydration number can be obtained by counting the number of ligands and water oxygen atoms in the first coordination shell of ions, respectively. Here, we define the radius of the first coordination shell of Na^+ ion to be 3.2 Å and monitor the change of coordination number and hydration number as a function of time for each ion in the selectivity filter. The results for $Site_{HFS}$ and $Site_{IN}$ are shown in Fig. 4C and D, respectively. For $Site_{HFS}$, both the coordination number and hydration number of Na^+ ion are found to vary mostly between 4 and 5 during the first 5.5 ns (Fig. 4C). Careful examination of the MD trajectory suggest that this Na^+ ion is located in the region well above the extracellular entrance of the selectivity filter and thus presents in a fully hydrated state (see Fig. 5B). After $t = 5.5$ ns, the Na^+ ion moves downward to the central region of

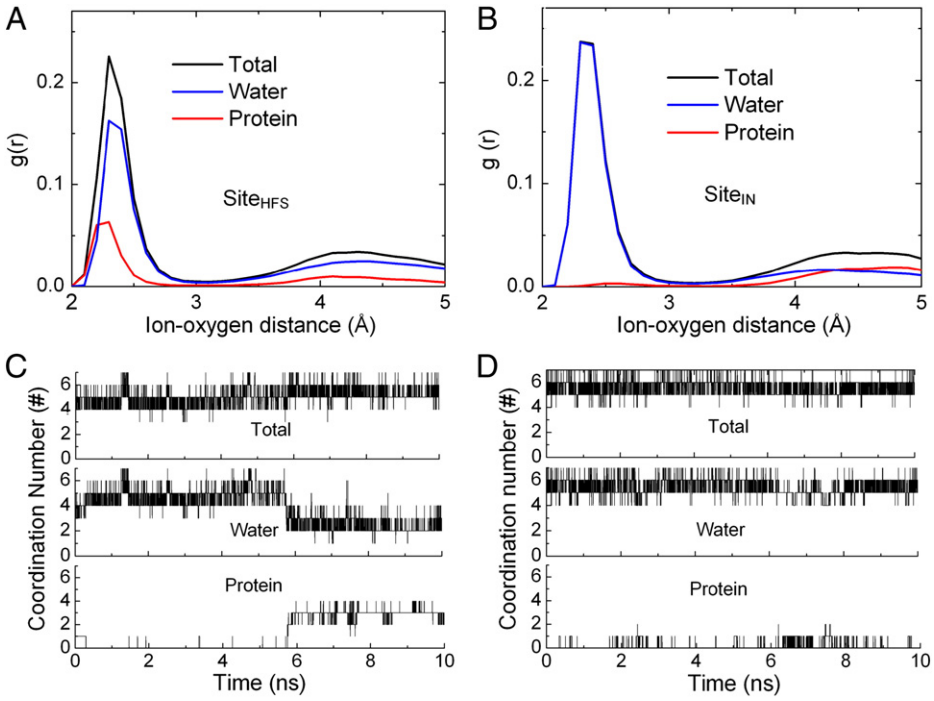

Fig. 4. Ion coordination state in the NavAb selectivity filter. (A, B) Ion-oxygen radial distribution function g(r) for Na^+ ions at $Site_{HFS}$ (A) and $Site_{IN}$ (B) with respect to total ligands (black), water oxygen (blue), and protein oxygen (red). (C, D) Coordination numbers of Na^+ ions at $Site_{HFS}$ (C) and $Site_{IN}$ (D) as a function of simulation time, respectively. Panels from top to bottom denote the coordination number for total ligands, for water oxygen atoms only (namely, the hydration number), and for protein oxygen atoms only, respectively.

$Site_{HFS}$ (see black line in Fig. 5A, and Fig. 5C) and its coordination number varies mostly between 5 and 6 (Fig. 4C, top panel) and surprisingly, the hydration number decreases significantly to ~3 (Fig. 4C, middle panel). Water oxygen atoms that originally bind with this Na^+ ion are replaced by about three oxygen atoms from the side chains of Glu177 (Fig. 4C bottom panel; Fig. 5C). This binding leads to a significant deflection of the Glu177 side chain toward the Na^+ ion, and thus results in the apparent increase in the RMSD profile of the selectivity filter (see Fig. 3, red and black curves). It is also shown that the side chains from only one or two out of the four protein monomers can simultaneously bind with the Na^+ ion and thus the ion is no longer located at the central axis of the channel pore (see Fig. 5C). The selectivity filter is also far from being symmetric, especially for the side chain of Glu177. This asymmetric ion binding manner that was not observed in K^+ channels may play a key role in controlling the transport properties of the NavAb channel. Different from $Site_{HFS}$, the coordination number and hydration number for Na^+ at $Site_{IN}$ are nearly identical during the entire 10 ns simulation (Fig. 4D, top and middle panels), consistent with the observation in the RDF profiles (Fig. 4B). This confirms that Na^+ ion at $Site_{IN}$ is nearly fully-hydrated. However, it should also be noted that the number of protein oxygen atoms within the coordination shell of this Na^+ does not change during our simulation (Fig. 4D, bottom panel), suggesting that Na^+ at this site can also asymmetrically bind to the protein, although with a low possibility. The oxygen providers for this coordination are the backbone carbonyl groups of the residue Leu176.

The demonstrated unique hydration pattern for Na^+ ions within the NavAb selectivity filter should be of great importance to the selectivity of this channel, which could be determined by measurements of relative permeability in electrophysiological experiments. The Na^+/K^+

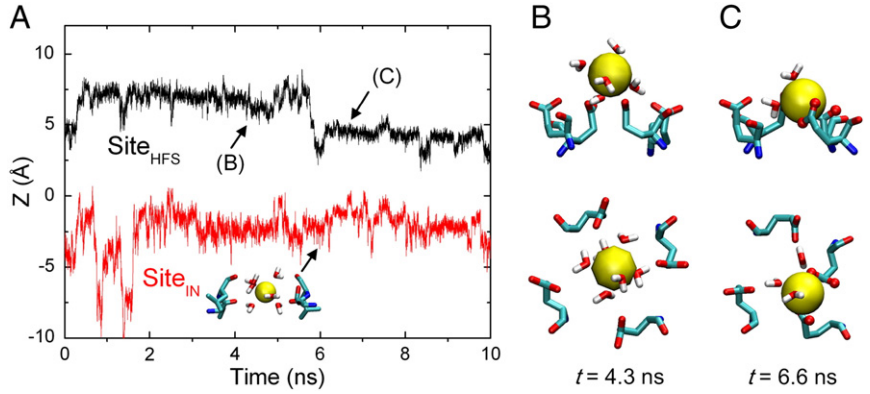

Fig. 5. Dynamics of Na^+ inside the NavAb selectivity filter. (A) The z trajectories (along the pore axis) of ions at $Site_{HFS}$ and $Site_{IN}$ in Sim6. Inset shows the coordination state of Na^+ at $Site_{IN}$. (B, C) Snapshots from MD simulation showing the side and top views of the coordination states of Na^+ at $Site_{HFS}$ with Glu177 side chains at $t = 4.3$ ns (B) and $t = 6.6$ ns (C), respectively. Na^+ ions, water oxygen and water hydrogen are shown in yellow, red and grey, respectively. The protein is shown in licorice representation, and the oxygen atoms of the Glu177 side chains that coordinate Na^+ ion are shown in red tiny spheres.

ion selectivity was suggested to originate from differences in relative free energies, which can be expressed as [27,56],

$$\Delta\Delta G\left[K^+ \rightarrow Na^+\right] = \Delta G_{pore}\left[K^+ \rightarrow Na^+\right] - \Delta G_{bulk}\left[K^+ \rightarrow Na^+\right].$$

Selectivity then arises when the difference in the ion's interaction energy with the coordinating ligands, $\Delta G_{pore}[K^+ \rightarrow Na^+]$, differs from the difference in their hydration energies, $\Delta G_{bulk}[K^+ \rightarrow Na^+]$. It was suggested that small changes in the number and/or the type of ligands involved in coordination of the ion have a big impact on the selectivity, which have been confirmed in the studies of K^+ and NaK channels [27]. Thus, the unique ion coordination state for NavAb channel should be of significance to its selectivity of Na^+ over K^+. During review of the manuscript, we learned of a study by Corry and Thomas, which suggested that the selectivity of Na^+ over K^+ in NavAb channel should result from the inability of K^+ to fit a plane of the Glu177 residues with the preferred solvation geometry, while smaller Na^+ can do this [57]. However, future extensive studies should be devoted into further clarifying this issue, due to the existence of significant thermal fluctuations of the Glu177 residue (~1.2 Å RMS) observed in our MD simulations, compared to the size difference between Na^+ and K^+ (~0.38 Å). It should be noted that, although the above discussion on channel selectivity focuses on energy minima (i.e., ion binding), previous electrophysiological experiments on the measurements of relative permeabilities from the Goldman–Hodgkin–Katz equation suggested that the entry barrier of ion permeation through channels also has a critical role in selectivity [4].

Fig. 5 shows the time evaluation of the Z trajectories of Na^+ ions at $Site_{HFS}$ and $Site_{IN}$. In K^+ [20,22] and NaK channels [29,30], ions were suggested to oscillate slightly within each binding site inside the selectivity filter. In contrast, large fluctuations are found for Na^+ ions inside the NavAb channel (Fig. 5). Especially, Na^+ ion at $Site_{IN}$ (red line) can even occasionally move to the cavity and shortly return to the binding site, showing the large degree of mobility of the ion at this site.

3.4. Ion conduction and potential of mean force through the selectivity filter

To study the ion conduction process across the NavAb channel, we performed five independent MD simulations with an electric field of 0.25, 0.5, 0.75 1.0 and 1.25 V/nm. For simplicity, we only consider the situation with one Na^+ ion at $Site_{IN}$ inside the selectivity filter. It is shown that when the applied electric field is less than 0.25 V/nm, no ion conduction was observed during 10 ns MD simulations. For the electric field of 0.5 V/nm, 0.75 V/nm, 1.0 V/nm and 1.25 V/nm, the conduction event takes place at 0.50 ns, 0.19 ns, 0.12 ns and 0.05 ns, respectively.

Fig. 6 shows the free energy for ion permeation through the selectivity filter of the NavAb channel. It is found that Na^+ inside the NavAb selectivity filter tends to bind at $Site_{IN}$, consistent with the above observation (see Table 1, Sim1–Sim3). The fact that Na^+ can easily transfer between this site and the cavity can also be confirmed by the free energy profile in which a weak energy barrier exists between these two ion binding sites. Ion movement from $Site_{IN}$ to $Site_{HFS}$ should overcome an energy barrier of ~1.8 kcal/mol. Furthermore, the occasional binding to the side chains of Glu177 yields an additional barrier of ~1.7 kcal/mol opposing Na^+ permeation. Furthermore, Na^+ experiences a huge energy barrier of ~8.42 kcal/mol to move from $Site_{HFS}$ to the bulk solution, suggesting that Na^+ ion is difficult to leave the selectivity filter and enter into the external solution. In real electrophysiological experiments, the energy barrier should be related to the single-channel current of the NavAb channel. The total barrier opposing Na^+ permeation through the NavAb channel is up to ~10.9 kcal/mol, and one can simply estimate the ion flux

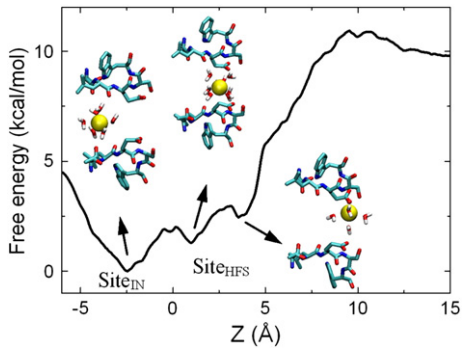

Fig. 6. One-dimensional potential of mean force for Na^+ conduction through the selectivity filter.

through the channel by the rate constant for crossing over this barrier [58]: $r = \nu(\exp[-G/kT])$, where G is the energy barrier, kT is the atomic thermal energy (0.593 kcal/mol at 298 K). The frequency factor, ν, is the value of rate constant when there is no energy barrier. If ion conduction occurs in a single-file manner, ν is often set to kT/h ($\sim 6\times10^{12}$ s^{-1} at biological temperatures; k, T, h are the Boltzmann constant, the absolute temperature and Planck constant, respectively.). The single-channel current can therefore be evaluated from its fundamental definition as the amount of charge that passes through the channel, per unit time, $J = qr$, where q is the charge of a single Na^+ ion (1.6×10^{-19} C). In terms of above calculations, the single-channel current for the NavAb channel is 9.9 pA. This value is 5 to 10-fold larger than the unitary currents measured for NaChBac (1–2 pA, depending on voltage and ionic conditions) [31], which are also typical values commonly observed for other Na^+ and K^+ channels. Several factors may account for this disagreement. First, only one ion inside the channel pore was considered, while under physiological conditions, ion conduction through the NavAb channel may adopt a multi-ion configuration, which will significantly change the energy landscapes governing Na^+ conduction. Second, the crystal structure we used in our simulations has a closed pore. In the case of an open one, the structure of the selectivity filter may be changed and thus the energy profile should be different. Third, the effect of the strength of membrane potential on the single-channel current is not taken into account explicitly in our estimation. In a real experimental measurement, the single-channel current should decrease monotonically with decreasing membrane potential. Finally, ion conduction in real situations occurs by overcoming a series of energy barriers, not only the dominant one used in our estimation. Clearly, further extensive experiments and simulations are required to address this issue, especially the direct measurement of single-channel current of NavAb.

4. Conclusions

In this study, extensive MD simulations of the NavAb channel with different ion configurations inside the channel pore were conducted. The RMSD results suggest that the protein is stable in all ion configurations we studied, and especially, the channel protein can even be stable without the presence of ions inside the selectivity filter. The robust stability we observed in NavAb channel is in sharp contrast to those of K^+ and NaK channels, in which the interior ions play key roles in stabilizing the structure of the channel protein. When Na^+ enters the NavAb selectivity filter, about two water molecules are dehydrated from the Na^+ coordination shell and replaced by the side chains of the residue Glu177 at $Site_{HFS}$. During this dehydrating process, only the side chains of Glu177 from one or two monomers out of the protein tetramer were found to contribute the ligands that coordinate the Na^+ ion, suggesting that this binding manner is asymmetric. Furthermore, our results also suggest that an applied electric field on Na^+ exceeding 0.5 V/nm will induce ion conduction across the selectivity filter. Further studies are required to address

in detail the energetics of ion conduction through the NavAb channel for different ion types such as K^+ and Ca^{2+} ions to unravel the selectivity mechanism of the channel.

Supplementary data to this article can be found online at http://dx.doi.org/10.1016/j.bbamem.2012.06.003.

Acknowledgement

This work is supported by the 973 Program (2012CB933403), the NSF (30970557, 91023026) of China, the Funding of Jiangsu Innovation Program for Graduate Education (CXLX11_0172) and the Fundamental Research Funds for the Central Universities.

References

[1] B. Hille, The permeability of the sodium channel to organic cations in myelinated nerve, J. Gen. Physiol. 58 (1971) 599–619.
[2] C.M. Armstrong, B. Hille, The inner quaternary ammonium ion receptor in potassium channels of the node of ranvier, J. Gen. Physiol. 59 (1972) 388–400.
[3] B. Hille, The permeability of the sodium channel to metal cations in myelinated nerve, J. Gen. Physiol. 59 (1972) 637–658.
[4] B. Hille, Potassium channels in myelinated nerve, J. Gen. Physiol. 61 (1973) 669–686.
[5] B. Hille, W. Schwarz, Potassium channels as multi-ion single-file pores, J. Gen. Physiol. 72 (1978) 409–442.
[6] T.M. Dwyer, D.J. Adams, B. Hille, The permeability of the endplate channel to organic cations in frog muscle, J. Gen. Physiol. 75 (1980) 469–492.
[7] C.M. Armstrong, Inactivation of the potassium conductance and related phenomena caused by quaternary ammonium ion injection in squid axons, J. Gen. Physiol. 54 (1969) 553–575.
[8] F. Bezanilla, C.M. Armstrong, Negative conductance caused by entry of sodium and cesium ions into the potassium channels of squid axons, J. Gen. Physiol. 60 (1972) 588–608.
[9] C.M. Armstrong, W.F. Gilly, Fast and slow steps in the activation of sodium channels, J. Gen. Physiol. 74 (1979) 691–711.
[10] D.A. Doyle, J.M. Cabral, R.A. Pfuetzner, A. Kuo, J.M. Gulbis, S.L. Cohen, B.T. Chait, R. MacKinnon, The structure of the potassium channel: molecular basis of K^+ conduction and Selectivity, Science 280 (1998) 69–77.
[11] Y. Zhou, J.H. Morais-Cabral, A. Kaufman, R. MacKinnon, Chemistry of ion coordination and hydration revealed by a K^+ channel-Fab complex at 2.0 Å resolution, Nature 414 (2001) 43–48.
[12] Y. Jiang, A. Lee, J. Chen, M. Cadene, B.T. Chait, R. MacKinnon, Crystal structure and mechanism of a calcium-gated potassium channel, Nature 417 (2002) 515–522.
[13] Y. Jiang, A. Lee, J. Chen, V. Ruta, M. Cadene, B.T. Chait, R. MacKinnon, X-ray structure of a voltage-dependent K^+ channel, Nature 423 (2003) 33–41.
[14] S.B. Long, E.B. Campbell, R. MacKinnon, Crystal structure of a mammalian voltage-dependent shaker family K^+ channel, Science 309 (2005) 897–903.
[15] J. Aqvist, V. Luzhkov, Ion permeation mechanism of the potassium channel, Nature 404 (2000) 881–884.
[16] B. Roux, Ion conduction and selectivity in K^+ channels, Annu. Rev. Biophys. Biomol. Struct. 34 (2005) 153–171.
[17] N. Shi, S. Ye, A. Alam, L. Chen, Y. Jiang, Atomic structure of a Na^+- and K^+-conducting channel, Nature 440 (2006) 570–574.
[18] A. Alam, Y. Jiang, High-resolution structure of the open NaK channel, Nat. Struct. Mol. Biol. 16 (2009) 30–34.
[19] T.W. Allen, S. Kuyucak, S.-H. Chung, Molecular dynamics study of the KcsA potassium channel, Biophys. J. 77 (1999) 2502–2516.
[20] I.H. Shrivastava, M.S.P. Sansom, Simulations of ion permeation through a potassium channel: molecular dynamics of KcsA in a phospholipid bilayer, Biophys. J. 78 (2000) 557–570.
[21] S. Berneche, B. Roux, Energetics of ion conduction through the K^+ channel, Nature 414 (2001) 73–77.
[22] I.H. Shrivastava, D. Peter Tieleman, P.C. Biggin, M.S.P. Sansom, K^+ versus Na^+ ions in a K channel selectivity filter: a simulation study, Biophys. J. 83 (2002) 633–645.
[23] O. Beckstein, P.C. Biggin, P. Bond, J.N. Bright, C. Domene, A. Grottesi, J. Holyoake, M.S.P. Sansom, Ion channel gating: insights via molecular simulations, FEBS Lett. 555 (2003) 85–90.
[24] S. Garofoli, P.C. Jordan, Modeling permeation energetics in the KcsA potassium channel, Biophys. J. 84 (2003) 2814–2830.
[25] M. Compoint, P. Carloni, C. Ramseyer, C. Girardet, Molecular dynamics study of the KcsA channel at 2.0-Å resolution: stability and concerted motions within the pore, Biochim. Biophys. Acta-Biomembr. 1661 (2004) 26–39.
[26] S.Y. Noskov, S. Berneche, B. Roux, Control of ion selectivity in potassium channels by electrostatic and dynamic properties of carbonyl ligands, Nature 431 (2004) 830–834.
[27] S.Y. Noskov, B. Roux, Importance of hydration and dynamics on the selectivity of the KcsA and NaK channels, J. Gen. Physiol. 129 (2007) 135–143.
[28] T. Baştuğ, S. Kuyucak, Comparative study of the energetics of ion permeation in Kv1.2 and KcsA potassium channels, Biophys. J. 100 (2011) 629–636.
[29] R. Shen, W. Guo, Ion binding properties and structure stability of the NaK channel, Biochim. Biophys. Acta-Biomembr. 1788 (2009) 1024–1032.
[30] R. Shen, W. Guo, W. Zhong, Hydration valve controlled non-selective conduction of Na^+ and K^+ in the NaK channel, Biochim. Biophys. Acta-Biomembr. 1798 (2010) 1474–1479.
[31] D. Ren, B. Navarro, H. Xu, L. Yue, Q. Shi, D.E. Clapham, A prokaryotic voltage-gated sodium channel, Science 294 (2001) 2372–2375.
[32] K. Charalambous, B.A. Wallace, NaChBac: the long lost sodium channel ancestor, Biochemistry 50 (2011) 6742–6752.
[33] Y. Zhao, T. Scheuer, W.A. Catterall, Reversed voltage-dependent gating of a bacterial sodium channel with proline substitutions in the S6 transmembrane segment, Proc. Natl. Acad. Sci. U. S. A. 101 (2004) 17873–17878.
[34] A. Kuzmenkin, F. Bezanilla, A.M. Correa, Gating of the bacterial sodium channel, NaChBac: voltage-dependent charge movement and gating currents, J. Gen. Physiol. 124 (2004) 349–356.
[35] L. Yue, B. Navarro, D. Ren, A. Ramos, D.E. Clapham, The cation selectivity filter of the bacterial sodium channel, NaChBac, J. Gen. Physiol. 120 (2002) 845–853.
[36] J. Payandeh, T. Scheuer, N. Zheng, W.A. Catterall, The crystal structure of a voltage-gated sodium channel, Nature 475 (2011) 353–358.
[37] V. Carnevale, W. Treptow, M.L. Klein, Sodium ion binding sites and hydration in the lumen of a bacterial ion channel from molecular dynamics simulations, J. Phys. Chem. Lett. 2 (2011) 2504–2508.
[38] W. Humphrey, A. Dalke, K. Schulten, VMD: visual molecular dynamics, J. Mol. Graph. 14 (1996) 33–38.
[39] L. Kale, R. Skeel, M. Bhandarkar, R. Brunner, A. Gursoy, N. Krawetz, J. Phillips, A. Shinozaki, K. Varadarajan, K. Schulten, NAMD2: greater scalability for parallel molecular dynamics, J. Comput. Phys. 151 (1999) 283–312.
[40] A.D. MacKerell, D. Bashford, M. Bellott, R.L. Dunbrack, J.D. Evanseck, M.J. Field, S. Fischer, J. Gao, H. Guo, S. Ha, D. Joseph-McCarthy, L. Kuchnir, K. Kuczera, F.T.K. Lau, C. Mattos, S. Michnick, T. Ngo, D.T. Nguyen, B. Prodhom, W.E. Reiher, B. Roux, M. Schlenkrich, J.C. Smith, R. Stote, J. Straub, M. Watanabe, J. Wiorkiewicz-Kuczera, D. Yin, M. Karplus, All-atom empirical potential for molecular modeling and dynamics studies of proteins, J. Phys. Chem. B 102 (1998) 3586–3616.
[41] W.L. Jorgensen, J. Chandrasekhar, J.D. Madura, R.W. Impey, M.L. Klein, Comparison of simple potential functions for simulating liquid water, J. Chem. Phys. 79 (1983) 926–935.
[42] B. Roux, S. Bernèche, On the potential functions used in molecular dynamics simulations of ion channels, Biophys. J. 82 (2002) 1681–1684.
[43] U. Essmann, L. Perera, M.L. Berkowitz, T. Darden, H. Lee, L.G. Pedersen, A smooth particle mesh Ewald method, J. Chem. Phys. 103 (1995) 8577–8593.
[44] S.E. Feller, Y. Zhang, R.W. Pastor, B.R. Brooks, Constant pressure molecular dynamics simulation: the Langevin piston method, J. Chem. Phys. 103 (1995) 4613–4621.
[45] O.S. Smart, J.G. Neduvelil, X. Wang, B.A. Wallace, M.S.P. Sansom, HOLE: a program for the analysis of the pore dimensions of ion channel structural models, J. Mol. Graph. 14 (1996) 354–360.
[46] F. Khalili-Araghi, E. Tajkhorshid, K. Schulten, Dynamics of K^+ ion conduction through Kv1.2, Biophys. J. 91 (2006) L72–L74.
[47] H.W. de Haan, I.S. Tolokh, C.G. Gray, S. Goldman, Nonequilibrium molecular dynamics calculation of the conductance of the KcsA potassium ion channel, Phys. Rev. E 74 (2006) 030905.
[48] W. Treptow, M. Tarek, K^+ conduction in the selectivity filter of potassium channels is monitored by the charge distribution along their sequence, Biophys. J. 91 (2006) L81–L83.
[49] D.B. Wells, S. Bhattacharya, R. Carr, C. Maffeo, A. Ho, J. Comer, A. Aksimentiev, Optimization of the molecular dynamics method for simulations of DNA and ion transport through biological nanopores, in: M.E. Gracheva (Ed.), Nanopore-Based Technology: Single Molecule Characterization and DNA Sequencing, Humana Press, Totowa, NJ, 2011.
[50] G.M. Torrie, J.P. Valleau, Nonphysical sampling distributions in Monte Carlo free-energy estimation: umbrella sampling, J. Comput. Phys. 23 (1977) 187–199.
[51] S. Kumar, J.M. Rosenberg, D. Bouzida, R.H. Swendsen, P.A. Kollman, The weighted histogram analysis method for free-energy calculations on biomolecules. I. The method, J. Comput. Chem. 13 (1992) 1011–1021.
[52] Y. Zhou, R. MacKinnon, The occupancy of ions in the K^+ selectivity filter: charge balance and coupling of ion binding to a protein conformational change underlie high conduction rates, J. Mol. Biol. 333 (2003) 965–975.
[53] A. Loboda, A. Melishchuk, C. Armstrong, Dilated and defunct K channels in the absence of K^+, Biophys. J. 80 (2001) 2704–2714.
[54] S. Bernèche, B. Roux, Molecular dynamics of the KcsA K^+ channel in a bilayer membrane, Biophys. J. 78 (2000) 2900–2917.
[55] M. Thomas, D. Jayatilaka, B. Corry, The predominant role of coordination number in potassium channel selectivity, Biophys. J. 93 (2007) 2635–2643.
[56] O.S. Andersen, Perspectives on: ion selectivity, J. Gen. Physiol. 137 (2011) 393–395.
[57] B. Corry, M. Thomas, Mechanism of ion permeation and selectivity in a voltage gated sodium channel, J. Am. Chem. Soc. 134 (2012) 1840–1846.
[58] E.W. McCleskey, Calcium channel permeation: a field in flux, J. Gen. Physiol. 113 (1999) 765–772.